Molecular Pharmacology Fast Forward. Published on February 11, 2016 as DOI: 10.1124/mol.116.103432
This article has not been copyedited and formatted. The final version may differ from this version.

Dipicrylamine modulates GABAρ1 receptors through interactions with residues in the TM4 and Cys-loop domains

Agenor Limon, Argel Estrada-Mondragón, Jorge M. Reyes Ruiz, Ricardo Miledi.

Neurobiology and Behavior, University of California, Irvine, 2205 McGaugh Hall, Irvine California 92697, United States. AL, JMRR, RM

Psychiatry and Human Behavior, University of California, Irvine, 2226 Gillespie NRF, Irvine California, 92697, Unites States. AL

The Queensland Brain Institute, QBI Building (number 79), St. Lucia, Queensland 4072, Australia. AEM

Molecular Pharmacology Fast Forward. Published on February 11, 2016 as DOI: 10.1124/mol.116.103432
This article has not been copyedited and formatted. The final version may differ from this version.

Running Title:

DPA effects on LGIC receptors

Corresponding author:

Agenor Limon,
2226 Gillespie NRF
Irvine CA; 92697-1675
alimonru@uci.edu

Number of text pages: 31

Tables: 1 in main text and 1 in Supplemental material

Figures: 8 in main text and 5 in Supplemental material

References: 42

Words in abstract: 250

Introduction: 380

Discussion: 1522

List of abbreviations:

$GABA_AR$s, $GABA_A$ receptors

DPA, dipicrylamine

LGIC, ligand gated ion channels;

BSA, bovine serum albumin

Molecular Pharmacology Fast Forward. Published on February 11, 2016 as DOI: 10.1124/mol.116.103432
This article has not been copyedited and formatted. The final version may differ from this version.

Abstract

Dipicrylamine (DPA) is a commonly used acceptor agent in Förster resonance energy transfer (FRET) experiments that allows the study of high frequency neuronal activity in the optical-monitoring of voltage in living cells. However, DPA potently antagonizes $GABA_A$ receptors ($GABA_ARs$) that contain α1 and β2 subunits by a mechanism which is not clearly understood. In this work, we aimed to determine whether DPA modulation is a general phenomenon of Cys-loop ligand-gated ion channels (LGICs) and whether this modulation depends on particular amino acid residues. For this we studied the effects of DPA on human homomeric GABAρ1, α7 nicotinic and $5\text{-}HT_{3A}$ receptors expressed in *Xenopus* oocytes. Our results indicate that DPA is an allosteric modulator of GABAρ1 receptors with an IC_{50} of 1.6 μM, an enhancer of α7 nicotinic receptors at relatively high concentrations of DPA, and has little, if any, effect on $5\text{-}HT_{3A}$ receptors. DPA antagonism of GABAρ1 was strongly enhanced by pre-incubation, was slightly voltage-dependent, and its washout was accelerated by bovine serum albumin. These results indicate that DPA modulation is not a general phenomenon of LGICs and structural differences between receptors may account for disparities in DPA effects. In silico modeling of DPA docking to GABAρ1, α7 nicotinic, and $5\text{-}HT_{3A}$ receptors suggests that a hydrophobic pocket within the Cys-loop and the M4 segment in GABAρ1, located at the extracellular/membrane interface, facilitates the interaction with DPA that leads to inhibition of the receptor. Functional examinations of mutant receptors support the involvement of the M4 segment in the allosteric modulation of GABAρ1 by DPA.

Molecular Pharmacology Fast Forward. Published on February 11, 2016 as DOI: 10.1124/mol.116.103432
This article has not been copyedited and formatted. The final version may differ from this version.

Introduction

Dipicrylamine (DPA) is a hydrophobic anion that intercalates into cellular membranes (Wang and Bruner, 1978) and has been broadly used as a probe to study the physical and biological properties of cellular membranes (Chanda et al., 2005; Kleijn et al., 1983; Oberhauser and Fernandez, 1995). Notably, DPA allows the study of high frequency neuronal activity in the optical-monitoring of voltage in living cells (Bradley et al., 2009); however, the compound's unexpected effects on $GABA_A$ receptors ($GABA_ARs$) and NMDA receptors have imposed limits on its broad physiological applications (Chisari et al., 2011; Linsenbardt et al., 2012). Thus, a better understanding of the mechanisms involved in DPA's effects would be helpful for effective modifications of the DPA molecule to reduce or eliminate its pharmacological activity while preserving its key optical characteristics. Thus far, the mechanism and specificity of the DPA inhibition of $GABA_ARs$ remains elusive (Chisari et al., 2011). Two non-mutually exclusive scenarios may explain DPA's effects. In one scenario, DPA may trigger unspecific local perturbations in the surrounding protein/lipid interphase that are responsible for conformational changes in the receptor and altered gating. In the other scenario, the antagonism is mediated by site-specific interactions between DPA and transmembrane sites of the receptor (Chisari et al., 2011; Mennerick et al., 2008).

To explore the potential mechanism for DPA's effects, we investigated whether DPA also affects human GABA receptors that are composed of ρ1 subunits (GABAρ1 receptors). The homomeric nature of this receptor is advantageous for structural modeling studies compared with heteromeric $GABA_ARs$ composed of GABA α, β, and γ subunits. After demonstrating that DPA also negatively modulates GABAρ1 receptors, we compared in silico structural models and the DPA inhibition of homomeric GABAρ1, α7 nicotinic receptors (nAChRα7), and $5\text{-}HT_{3A}$

Molecular Pharmacology Fast Forward. Published on February 11, 2016 as DOI: 10.1124/mol.116.103432
This article has not been copyedited and formatted. The final version may differ from this version.

receptors to identify structural motifs with the potential to interact with DPA. Finally, we performed a mutagenesis analysis of the GABAρ1 subunit to determine the congruence between the structural model and DPA effects. Our results demonstrate that DPA is an allosteric modulator of $GABA_A$Rs and exhibits pharmacological effects on α7 nicotinic ACh receptors but little, if any, effects on 5-HT_{3A} receptors. The aromatic residue W475, which is located in the upper part of the transmembrane domain 4 (TM4) of GABAρ1, appears to participate in the gating of the receptor and in the DPA-mediated inhibition of GABAρ1 receptors.

Materials and Methods

Molecular biology

For the experiments using $GABA_A$Rs, we used mRNA that was isolated from rat brain cortices using the FastTrack 2.0 kit (Invitrogen, Carlsbad, CA). For the expression of homomeric channels, we used human α7 nicotinic receptor cDNA (donated by Professor Eleonora Palma; Universita di Roma La Sapienza), human 5-HT_{3A} cDNA (purchased from Missouri S&T cDNA Resource Center), and GABAρ1, which was cloned from a human retina cDNA library (Martinez-Torres et al., 1998), and introduced the genes into pcDNA3 (Invitrogen, Carlsbad, CA). These plasmids were transformed into the *Escherichia coli* DH5α strain for storage and amplification. Linearized plasmids were used as templates for cRNA synthesis using the Ambion's mMessage mMachine kit (Ambion, Austin, TX). Stage V−VI *Xenopus* oocytes were injected with 50 nl of mRNA or cRNA (concentration of 1 mg/mL) and then maintained in Barth's solution [88 mM NaCl, 0.33 mM $Ca(NO_3)_2$, 0.41 mM $CaCl_2$, 1 mM KCl, 0.82 mM $MgSO_4$, 2.4 mM $NaHCO_3$, 10 mM HEPES (pH 7.4)] with 100 U/mL of penicillin and 0.1 mg/mL of streptomycin (Sigma; St Louis, MO) at 16-17 °C until the moment of recording.

Molecular Pharmacology Fast Forward. Published on February 11, 2016 as DOI: 10.1124/mol.116.103432
This article has not been copyedited and formatted. The final version may differ from this version.

Electrophysiological assay

The oocytes were harvested and prepared as previously described (Miledi et al., 2006), with slight modifications as noted below. Briefly, *Xenopus laevis* frogs were anesthetized in tricaine methane sulfonate (MS-222, 0.17%) and euthanized by decapitation, in adherence to protocols approved by the University of California Institutional Animal Care and Use Committee. The ovarian lobes were removed, cut into small pieces and placed in Ca^{2+}-free Barth's solution with 2 mg/ml collagenase type I (Sigma) for 2 hr in constant rotation. After the enzymatic treatment, isolated stage V–VI oocytes were selected and maintained at 17 °C for the remainder of the experiment. Healthy looking oocytes were injected approximately 24 hr after enzymatic dissociation. Three to four days after injection, the oocytes were impaled with two microelectrodes filled with 3 M KCl and voltage clamped at -80 mV using a two-electrode voltage clamp amplifier (Miledi, 1982). The oocytes were continuously perfused with gravity-driven frog Ringer's solution [115 mM NaCl, 2 mM KCl, 1.8 mM $CaCl_2$, 5 mM HEPES (pH 7.4)] at room temperature (19−21 °C). Data acquisition was performed using WinWCP V 3.9.4 (John Dempster, Glasgow, United Kingdom), as previously reported (Limon et al., 2010; Ochoa-de la Paz et al., 2012). DPA was purchased from Biotium (Hayward, CA). The rest of the substances used were obtained from Sigma-Aldrich (St. Louis, MO).

Data analysis

The antagonist effect of DPA on GABA currents was determined by measuring the percent inhibition produced by different concentrations of DPA. The concentration of DPA causing a 50% decrease in GABA currents (IC_{50}) was estimated by fitting the following logistic equation to the experimental data: $I = I_{min} + (I_{max} - I_{min})/[1 + (x/IC_{50})k]$ (Origin 8.5), in which x is

Molecular Pharmacology Fast Forward. Published on February 11, 2016 as DOI: 10.1124/mol.116.103432
This article has not been copyedited and formatted. The final version may differ from this version.

the concentration of DPA (in M), *I* is the amplitude of the agonist response (in nA), and k is the slope of the curve. The EC_{50} and the Hill coefficient were determined by fitting the Hill equation in the form $I = I_{max}/(1+(EC_{50}/[A])^n)$, in which *I* is the current amplitude, I_{max} is the maximum current amplitude at the concentration of the agonist [A], EC_{50} is the agonist concentration that induces 50% of the maximal response, and *n* is the Hill coefficient. The time constants of activation and deactivation were measured by fitting a simple exponential equation between the 10-90% of the rise and decay current using Clampfit v.10.0 software (Molecular Devices). The experimental data are shown as the mean ± S.E.M. Statistical differences were determined by Student's *t*-test when comparing a pair of responses and by Dunnett's test when making multiple comparisons with respect to the GABAρ1 wild type receptor (WT) (JMP v. 10; SAS Institute). We considered two groups significantly different when $P < 0.05$.

Homology modeling

Three homology models of the GABAρ1, α7 nicotinic and 5-HT_{3A} subunits were built. The first model was based on the recently published structure of the β3 homomeric human $GABA_A$ receptor (PDB code 4COF, (Miller and Aricescu, 2014)), and the last two models used the structure of the nicotinic acetylcholine receptor from the *Torpedo marmorata* electric organ (PDB code 4AQ9, (Unwin and Fujiyoshi, 2012)). We employed MODELLER v9.12 (Sali and Blundell, 1993) and built 20 models of each subunit by applying the respective alignments of the UniProt code sequences: P24046 (GABA ρ1), P36544 (α7 nicotinic), and P46098 (5-$HT3_A$) (Supplementary Figures 1 and 2). Then, in each case, we chose the best model based on the TM score and RMSD.

Each subunit was then projected five-fold onto their respective template using Molsoft ICM-Pro v3.5 (Totrov and Abagyan, 1997), and the few clashes observed at the interfaces were

Molecular Pharmacology Fast Forward. Published on February 11, 2016 as DOI: 10.1124/mol.116.103432
This article has not been copyedited and formatted. The final version may differ from this version.

removed by local energy minimization. The entire pentamers were refined by energy minimization using the internal coordinate space, followed by optimizing the geometry of the built structures with a fast Dreiding-like forcefield employing Accelrys Discovery Studio v2.5 (Chen et al., 2006). The human GABAρ1 subunit is 52%, 56% and 61% homologous to the GABA subunits α1 (Uniprot P14867), γ2L (Uniprot P18507) and β3 (Uniprot P28472), respectively. Because the structure of the homomeric β3 GABA receptor was recently solved (Miller and Aricescu, 2014) and GABA ρ1 and β3 form homomeric receptors and have high homology we think that using β3 as a template can give us a better estimation about the physiological and molecular aspects of the receptor interacting with dipicrylamine.

Molecular docking

We used Pocket Finder in ICM, as previously reported (Dey and Chen, 2011). Briefly, three (GABAρ1), four (α7 nicotinic), or eight (5-HT3$_A$) sites per subunit were identified by the automatic detection of small molecule binding sites on the homomeric receptors (Supplemental Figure 3); then, one copy of the 3D structure of DPA (2,4,6-trinitro-N-(2,4,6-trinitrophenyl)aniline) was loaded from ChemSpider into the ICM project (CSID:8258, http://www.chemspider.com/Chemical-Structure.8258.html). The estimated octanol/water partition coefficient of DPA (log Kow = 3.35) indicates that the compound would be poorly soluble in water; thus, we only considered sites that were located at the extracellular/membrane interface (II in GABAρ1; I in α7 nicotinic; and II and III in 5-HT3$_A$) as putative sites for allosteric modulation. One or two molecules were accommodated in each pocket by applying a second local energy minimization. The same procedure was done to dock DPA molecule to the

Molecular Pharmacology Fast Forward. Published on February 11, 2016 as DOI: 10.1124/mol.116.103432
This article has not been copyedited and formatted. The final version may differ from this version.

heteromeric model of $GABA_A$ receptor. The images were made using ICM and PyMOL v 1.5.0.4.

Results

DPA's effects on $GABA_ARs$

To determine whether the DPA antagonism originally described for the α1β2 and α1β2γ2 $GABA_ARs$ extends to other endogenous $GABA_ARs$ we evaluated DPA effects on oocytes that were previously injected with mRNA isolated from rat brain cortex. These mRNA-injected oocytes express a large variety of $GABA_ARs$ that are representative of those expressed in the rat brain (Demuro et al., 1999). To ensure maximum activation of all subtypes of mRNA-expressed $GABA_ARs$ we tested DPA with saturating concentrations of GABA. In agreement with Chisari et al., the coapplication of GABA and DPA reduced the peak and accelerated the decay of GABA currents in a concentration-dependent manner (Fig. 1A, C). This result indicates that the DPA antagonism described for α1β2 and α1β2γ2 $GABA_ARs$ is qualitatively similar in $GABA_ARs$ that were expressed by endogenous rat brain mRNA. Notably, the recovery from DPA inhibition was not complete even after 30 min; therefore, to avoid cumulative effects on the concentration response experiments, each oocyte was tested with DPA only once. The IC_{50} of the aqueous DPA concentration was 62 ± 11 nM (n = 3–5 oocytes per concentration), which is a value similar to that reported for the DPA inhibition of $GABA_ARs$ with α1β2γ2 stoichiometry (65 nM) (Chisari et al., 2011).

DPA antagonism of homomeric GABAρ1 receptors

GABAρ1 receptors exhibit a high affinity for GABA, demonstrate slow desensitization and have a pharmacological profile so distinctive that for approximately two decades they were classified

Molecular Pharmacology Fast Forward. Published on February 11, 2016 as DOI: 10.1124/mol.116.103432
This article has not been copyedited and formatted. The final version may differ from this version.

as $GABA_C$ (Martinez-Delgado et al., 2010). Therefore, we investigated whether GABAρ1 receptors were modulated by DPA. Figure 1B-C shows that the coapplication of DPA and GABA inhibited the maximal response of GABAρ1 receptors with an IC_{50} of 1.57 ± 0.2 μM (n = 4). The effects of DPA on GABAρ1 kinetics were different than those observed on $GABA_A$Rs from rat brain cortices (Fig. 1A) and heterologously expressed α1β2γ2 receptors (Chisari et al., 2011). The GABAρ1 receptors exhibited a tail current at the end of the GABA and DPA coapplication (Fig. 1B), indicating that inhibition by DPA is partially relieved faster than the deactivation of GABAρ1 channels is completed.

DPA also produced a 5-fold dextral displacement of the concentration/response curve for GABA (Fig. 2), increasing the EC_{50} from 0.91 ± 0.3 μM to 4.59 ± 1.6 μM (n = 3–5 oocytes per point; p = 0.031; Fig. 2A, B), and a reduction of the Hill coefficient from 2.34 ± 0.3 to 1.07 ± 0.25 (p = 0.001). DPA antagonism was not surmounted by increasing the concentration of GABA, a result that is consistent with the non-competitive, negative allosteric modulation of the GABAρ1 receptor (Fig. 2B). Notably, the antagonism of the GABAρ1 receptor was enhanced by preincubation with DPA. Without preincubation, the coapplication of 5 μM DPA and GABA reduced the maximum current by 15 ± 3% (n = 5; Fig. 2B, black triangle); however, when DPA was preincubated for 3 min, the GABA efficacy was reduced by 91.1 ± 1.7% (n = 5; white triangles in Fig. 2B), indicating that the DPA antagonism of $GABA_A$R has a slow onset rate. Given the effects of DPA preincubation on GABA efficacy we also studied the effect of 3 μM DPA, preincubated by 200 s, on the concentration/response dependence of GABAρ1 receptors (Fig. 2B). In this condition 3 μM DPA reduced the maximal GABA efficacy by 77 ± 6.6% and doubled the EC_{50} for GABA from 0.91 in control to 2.0 ± 0.16 μM (n = 4 oocytes; p = 0.021), without affecting the Hill coefficient (2.34 to 1.9 ± 0.14; n = 4 oocytes, p = 0.263).

Molecular Pharmacology Fast Forward. Published on February 11, 2016 as DOI: 10.1124/mol.116.103432
This article has not been copyedited and formatted. The final version may differ from this version.

Further experiments demonstrated that the percentage of DPA inhibition exponentially increased, with the incubation time reaching a maximum after approximately 3 min (Fig. 3A, B). The percentage of maximal inhibition was greater when the oocytes were tested with DPA only once (91.1 ± 1.7%; Fig. 3A, B) than when they were tested consecutive times (maximum inhibition of 42.4 ± 7.6%; n = 4; data not shown), suggesting incomplete recovery from DPA's effects between applications, even after washout periods of more than 20 min. Chisari et al., previously reported that bovine serum albumin (BSA) a molecular scavenger of DPA accelerated DPA membrane removal and the antagonism offset of $GABA_A$Rs (Chisari et al., 2011); therefore, we analyzed whether a similar mechanism was present in DPA antagonism of GABAρ1. In our experiments BSA also accelerated DPA washout (Fig. 3C, D) reducing the τ of antagonism offset from 36.2 ± 5.3 s in absence of BSA to 16.8 ± 1.7 s in presence of BSA ($p = 0.014$; n = 4). This result indicates that incomplete recovery of DPA can be explained by incomplete DPA membrane removal.

Voltage dependence of DPA inhibition

Partitioned DPA is negatively charged and generates charge movements when translocating within the plasma membrane in response to changes in voltage. Previous studies have indicated that DPA's charge movements in oocyte membranes can be described by a Boltzmann function with $V_{1/2}$ for oocytes of -54 and -59 mV for injected and uninjected oocytes, respectively (Chisari et al., 2011), we performed similar experiments in non-injected oocytes and obtained a $V_{1/2}$ of -55 ± 2.3 mV (n = 6) (Figure 4A). Therefore, we investigated whether the effects of DPA on GABAρ1 also varied with changes in voltage. For this study, we exploited the slow desensitization of GABAρ1-mediated currents that facilitate the use of voltage ramp protocols to measure the effects of DPA on steady-state currents. A steady-state GABA current was obtained

Molecular Pharmacology Fast Forward. Published on February 11, 2016 as DOI: 10.1124/mol.116.103432
This article has not been copyedited and formatted. The final version may differ from this version.

by subtracting the current elicited by a voltage ramp protocol from -90 mV to +65 mV (80 mV/s) under control conditions from the ramp-elicited current after the response to 1 μM GABA reached an equilibrium (Figure 4). The sensitivity of any oocyte's endogenous component to 3 μM DPA was determined by subtracting the ramp-elicited currents before and after 200 s of incubation with DPA. The fraction of steady-state GABA current available after 200 s of 3 μM DPA preincubation was obtained by subtracting ramp-elicited currents with DPA from those elicited during the coapplication of 3 μM DPA and 1 μM GABA.

The inversion potential of GABA currents (E_{GABA}) before and after DPA was -25.4 ± 3.1 mV and -21.8 ± 1.6 mV, respectively, indicating that DPA did not affect the permeability of the channel (n = 5, p = 0.33). We did observe a small but significant voltage dependence for DPA modulation of the GABAρ1 receptor. Figure 4C shows that the percentage of inhibition of the GABA current linearly decreased with positive voltages between 0 and +60 mV ($r^2 = 0.99$); however, at negative voltages down to -60 mV, the percentage of inhibition remained unchanged, regardless of the voltage. We did not extend the voltage ramp protocol beyond +65 mV because more positive voltages are not normally observed in physiological conditions. Moreover, because the percentage of inhibition trends asymptotically to ± ∞ when close to E_{GABA}, we excluded from the analysis the voltage range in which the percentage of inhibition could not be reliably calculated. For comparison purposes, we calculated the DPA-mediated inhibition of the steady-state GABA current at -90 and +50 mV. As observed in Figure 4, DPA reduced the steady-state GABA current to 20.1 ± 5.3% and 35 ± 5.1% of the control at -90 and + 50 mV, respectively (n = 5, p < 0.001, paired Student's *t*-test). Additionally, we also measured the onset rate of DPA antagonism at -90 and +50 mV once the current was already activated. Figure 4E-G shows that DPA inhibition of the GABA current was faster at -90 mV than at +50

Molecular Pharmacology Fast Forward. Published on February 11, 2016 as DOI: 10.1124/mol.116.103432
This article has not been copyedited and formatted. The final version may differ from this version.

mV. The best fit for the onset of DPA's effects was the sum of two exponential functions with the time constants τ_1 2.0 ± 0.9 s and τ_2 9.6 ± 1.6 s at -90 mV (n = 5) and τ_1 2.3 ± 0.1 s and τ_2 16.9 ± 1.8 s at +50 mV (n = 5). τ_2 was significantly slower at positive voltages ($p < 0.05$, Student's *t*-test) (Fig. 4F).

Previous studies, and our own results, indicate that DPA's charge movements in oocyte membranes can be described by a Boltzmann function with $V_{1/2}$ of approximately -54 mV; therefore, at membrane potentials of -90 mV, the concentration of DPA is expected to be higher in the outer leaflet of the plasma membrane. The faster onset of DPA antagonism at negative potentials suggests that inhibition is favored when DPA molecules are near the protein-lipid interface at the upper part of the receptor. In addition, depolarization during ramp protocols should translocate free or weakly bound DPA with a $V_{1/2}$ of approximately -55 mV; however, our experiments indicate that a partial removal of steady-state antagonism is observed at values more positive than 0 mV. This result suggests that depolarizing voltages are not sufficient to counter a) the affinity of DPA for the activated receptor and/or b) the slow kinetics of DPA dissociation (see below in discussion).

DPA effects on homomeric receptors of the LGIC family

The GABA ρ1 and α1 subunits are only 33% homologous, and receptors containing either of these subunits exhibit profound pharmacological differences. Nevertheless, ρ1 and α1β2 GABA receptors are both antagonized by DPA. Based on the effects of DPA on GABAρ1, we hypothesized that if DPA also modulated other homomeric members of the Cys-loop LGIC family, then we could perform comparative studies between the functional effects of DPA and

Molecular Pharmacology Fast Forward. Published on February 11, 2016 as DOI: 10.1124/mol.116.103432
This article has not been copyedited and formatted. The final version may differ from this version.

the structure of those receptors. Therefore, we evaluated the effects of DPA on homomeric 5-HT_{3A} and α7 nicotinic receptors.

DPA did not significantly modify the maximal response of 5-HT_{3A} receptors elicited by a high concentration of 5-HT (10 μM) (Fig. 5); small changes in the desensitization of 5-HT-elicited currents were not significant upon statistical testing ($P > 0.05$, paired Student's *t*-test). By contrast, α7 nicotinic receptors were modulated by high concentrations of DPA. Whereas 1 μM DPA exhibited almost no effect on maximal α7 nicotinic receptor responses elicited by a saturating concentration of ACh (100 μM) (97 ± 8% of control; n = 5), 5 μM DPA increased the peak of ACh-elicited currents by 91 ± 15% (n = 12; Fig. 5). The potentiation of α7 nicotinic receptors by DPA was observed only for the current activation, with no effect on the desensitization.

In silico modeling of a binding domain for DPA in homomeric receptors of the LGIC family

The differential effects of DPA on GABAρ1, α7 nicotinic and 5-HT_{3A} homopentameric receptors provided an opportunity to further examine the structural components of the receptors that might interact with DPA. We created an in silico model of each receptor. Each model displayed a different pattern of potential pockets that can interact with DPA throughout their extracellular and transmembrane domains, according to their particular architecture. Because the partition coefficient of DPA predicts poor solubility in water, we only considered sites that were located at the extracellular/membrane interface as putative sites for allosteric modulation in each case. The 5-HT_{3A} receptor contains two sites that are each able to accommodate one molecule of DPA, whereas the GABAρ1 and α7 nicotinic receptors display enough space to contain just one molecule at the protein-lipid interface in each subunit (sites II in GABAρ1, I in α7 nicotinic, and

Molecular Pharmacology Fast Forward. Published on February 11, 2016 as DOI: 10.1124/mol.116.103432
This article has not been copyedited and formatted. The final version may differ from this version.

II and III in 5-HT3$_A$; Supplemental Figure 3). These sites were located in the upper half of the transmembrane domain near the superior limit of the membrane in all of the models (Figure 6).

We identified several hydrophobic aromatic residues interacting with DPA in the three models and/or positively charged arginine residues in the GABAρ1 and α7 nicotinic receptors. These residues include L207, I281, L285, Y289, Y474, and W475 in GABAρ1; F157, F159, R227, Y296, F297, and F493 in α7 nicotinic receptors; and F166, F164, F309, and W472 in the 5-HT$_{3A}$ receptors (Figure 6). The pattern appears to indicate the existence of certain acidic recognition motifs rich in aromatic, hydrophobic and even positively charged amino acids that provide π-stacking and electrostatic contributions to stabilize the structure of DPA. This conserved pocket formed by amino acids in the Cys-loop, M1 and M4 domains is reminiscent of the general anesthetic cavity that was reported by Nury et al. (Nury et al., 2011), notwithstanding that the specific residues that interact in each case induce a very different physiological response. Previous results demonstrated that a point mutation in the transmembrane domain 2 of the α1 subunit (V256S) that renders α1β2 and α1β2γ2 receptors insensitive to pregnenolone sulfate (PS)(Akk et al., 2001) also removes sensitivity to DPA(Chisari et al., 2011). Akk et al., originally described the mutation and concluded that this residue is unlikely to be part of the binding site for PS and may influence PS action indirectly. In agreement with that interpretation, our model of GABAρ1 does not predict interactions between the DPA and the residue equivalent to V256 in α1β2.

Interactions between DPA and in silico heteromeric α1β2γ2 GABA$_A$ receptor

To explore possible interactions between V256 and DPA in heteromeric GABA receptors we used a model of α1β2γ2 (Estrada-Mondragon and Lynch, 2015)(Supplemental Figure 4), in this

Molecular Pharmacology Fast Forward. Published on February 11, 2016 as DOI: 10.1124/mol.116.103432
This article has not been copyedited and formatted. The final version may differ from this version.

model V256 in α1β2γ2 does not interact with DPA indicating that V256 is most likely involved in the signal transduction mechanisms following binding by DPA to another site. We also explored hydrophobic pockets in the α1β2γ2 model; interestingly, α1 and ρ1 subunits share the same pattern of interactions with DPA, with basically the same equivalent residues able to accommodate one DPA molecule in the hydrophobic pocket (Supplemental Figure 4). In the other hand, γ2 and β2 are able to accommodate two DPA molecules each; however, the interactions resemble more those described for the 5-HT_{3A} receptor, where the impact in the function is minimal. Our model predicts that interactions of DPA with the α1 subunit are strong drivers of non-competitive antagonism of DPA in heteromeric $GABA_A$ receptors. These interactions do not discard that additional non-specific membrane perturbations also participate in the inhibition of these receptors. Future comparative studies between heteromeric and homomeric $GABA_A$ receptor should provide more information regarding the differences in DPA antagonism between these receptors.

DPA effects on GABAρ1 receptors with structural modifications on M4

Because amino acids at the end of the M4 domain appear to be important for DPA binding and because interactions between M4 and the Cys-loop are necessary for channel activation (Estrada-Mondragon et al., 2010), we studied the effects of the DPA-mediated antagonism of GABAρ1 receptors mutated in the M4 domain.

We tested the effects of DPA on GABAρ1 mutants in which the C-termini of the M4 was shortened by 1 (S479X or GABAρ1-1aa), 2 (F478X or GABAρ1-2aa), or 3 (I477X or GABAρ1-3aa) amino acids (Reyes-Ruiz et al., 2010). These mutants exhibited clear changes in their

Molecular Pharmacology Fast Forward. Published on February 11, 2016 as DOI: 10.1124/mol.116.103432
This article has not been copyedited and formatted. The final version may differ from this version.

kinetic properties when activated with GABA (Reyes-Ruiz et al., 2010). Whereas the deletion of 1 amino acid slowed the activation and decay of the current, the deletion of 2 amino acids greatly accelerated both parameters (Table 1), suggesting a close involvement of the M4 end termini in the gating of the GABAρ1 receptor. To test the effects of DPA, we preincubated the receptors with 1 μM DPA for 180 s and then co-treated them with DPA and the EC_{50} concentration of GABA for each receptor subtype (see Table 1); this procedure allows for the maximal antagonism of DPA at the EC_{50} while reducing acute nonspecific effects of DPA on the membrane. Using this procedure, we found that the deletion of up to 2 amino acids did not affect DPA-mediated antagonism (Fig. 7). However, DPA antagonism was modestly enhanced in the -3aa mutant, blocking GABA currents by 76.4 ± 1.3% in GABAρ1-3aa vs. 68.7 ± 0.9% in WT ($n = 6$; $p = 0.002$; Fig. 7).

The amplitude of the post-DPA current tail was positively correlated with the decay time of the GABA currents ($r = 0.93$; Supplemental Figure 5). The largest tail was observed in GABAρ1-1aa and was absent in GABAρ1-2aa; these were the mutants with the highest and lowest deactivation time constants, respectively (Fig. 7 and Table 1). This result indicates that the post-DPA tail arises from speed differences in GABA current decay and relief from DPA antagonism. Further shortening of M4 produced nonfunctional receptors (Reyes-Ruiz et al., 2010).

Next, we examined the role of the residue W475 that our model implicated in the charge stabilization of DPA within the hydrophobic pocket of each GABAρ1 subunit. As previously demonstrated, the substitution of W475 by electrically charged amino acids (W475R and W475D) produced nonfunctional receptors, indicating the fundamental role of W475 in the gating of the receptor (Estrada-Mondragon et al., 2010). The substitution of W475 with

Molecular Pharmacology Fast Forward. Published on February 11, 2016 as DOI: 10.1124/mol.116.103432
This article has not been copyedited and formatted. The final version may differ from this version.

hydrophobic amino acids (W475F, W475L, W475G, and W475A) produced functional channels with less sensitivity and lower efficacy in response to GABA and faster kinetics, and all of the mutants except W475L demonstrated less cooperativity (as reported by the Hill coefficient) than the WT receptor (Table 1). Despite the differences in kinetic and affinity properties between mutants and the WT receptor, we did not observe a statistically significant difference in the antagonistic activity of DPA against W475F, W475L, and W475G with respect to the WT receptor; however, W475A was less sensitive to DPA than the WT receptor (Fig. 7). The IC_{50} for DPA antagonism, measured after 3 min preincubation with DPA, of W475A's EC_{50} was significantly higher (843 ± 35 nM; n = 4, $p < 0.001$, Dunnett's method) than that for W475F (383 ± 38 nM; n = 4) and WT (309 ± 30 nM; n = 4).

Discussion

In this study we report for first time that DPA is a negative allosteric modulator of GABAρ1 and a potentiator of α7 nicotinic receptors, with no detectable effects on $5\text{-}HT_{3A}$ receptors. The differential pharmacological effects of DPA on distinct receptors of the Cys-loop LGIC family are supportive of a mechanistic model in which DPA modulates receptor activity via site-specific interactions located within transmembrane segments.

Interactions between DPA and in silico homomeric LGIC channels

By using the recently published structure of the anionic β3 homomeric human $GABA_AR$ (Miller and Aricescu, 2014), we adjusted the previous GABAρ1 model (Estrada-Mondragon et al., 2010), which now exhibits a higher alignment score in homology and identity (Supplemental Figures 1 and 2). Our new GABAρ1 model predicts interactions between the DPA molecule and

Molecular Pharmacology Fast Forward. Published on February 11, 2016 as DOI: 10.1124/mol.116.103432
This article has not been copyedited and formatted. The final version may differ from this version.

several residues located in the upper half of the transmembrane domain to form a hydrophobic cavity that encages DPA in a very stable conformation. This hydrophobic cavity is located behind the upper part of the pore. Recent progress in the search of the gating mechanism along the channel indicates that the upper half of the pore that is lined by the M2 domain of each subunit undergoes considerable deformation, being functionally coupled through loop M2-M3 with loop 2 of the extracellular domain during ligand-induced activation (Prevost et al., 2012; Unwin and Fujiyoshi, 2012). Lipids contribute in a fundamental way to achieve this coupling through critical points conferred by few hydrophobic residues and by electrically charged residues in such interphases (daCosta et al., 2009; Estrada-Mondragon et al., 2010; Fernandez Nievas et al., 2008). Our previous studies have demonstrated that at least two amino acids that form the hydrophobic cavity for DPA, W475 in TM4, and L207 in the Cys-loop participate in planar hydrophobic interactions that are necessary for the activation of the GABAρ1 channel (Estrada-Mondragon et al., 2010); therefore, the presence of DPA inside the hydrophobic pocket may hinder physiological TM4-Cys-loop interactions, which in turn alter the gating of the channel (see below).

A similar cavity was identified in α7 nicotinic receptors, wherein an entire hydrophobic aromatic network distributed along the neighboring pre-TM1 and Cys-loop domains appears to interact with DPA. Based on the potentiation effects elicited by DPA, DPA interactions in this cavity may promote energetic coupling stacking by narrowing the distance between the aromatic residues in the TM1 and Cys-loop domains and those in the TM2-TM3 domain because the participation of inter-residue coupling in these domains is known to be important for rapid and efficient gating of the nicotinic receptor, as described by (Lee et al., 2009).

Molecular Pharmacology Fast Forward. Published on February 11, 2016 as DOI: 10.1124/mol.116.103432
This article has not been copyedited and formatted. The final version may differ from this version.

In the case of the cationic 5-HT_{3A} receptor, the interface between extracellular and transmembrane domains appears to be quite different from those of anionic LGIC receptors and even significantly different from cationic receptors such as α7 nicotinic receptors (Bouzat et al., 2008). Certain charged residues that have been identified as key elements for channel activation, such as R241 in the pre-TM1 domain (Hu and Peoples, 2008; Hu et al., 2003) and K76 in loop 2 (Reeves et al., 2005), are located a considerable distance away from the docked position of DPA molecules in our model. In fact, these regions are only stabilized loosely by hydrophobic residues close to the membrane upper leaflet and are substantially distant from any charged residue. The lack of DPA effects on the 5-HT_{3A} receptor indicates that the presence of the hydrophobic pocket where DPA fits is not enough requirement for antagonism; in addition, appropriate stabilization of DPA's charge and interaction with amino acids involved in gating of the channel is necessary for allosteric modulation by DPA.

We propose that although the interface of interaction is very similar among the different receptors, the specificities of each receptor induce a very different response, which fits well and complements the data presented here.

Allosteric modulation of GABAρ1 by DPA

Our GABAρ1 model suggests that bound DPA alters the gating of the channel by affecting interactions between W475 in TM4 and L207 in the Cys-loop domains. Evidence of allosteric modulation and gating alterations is further provided by the exponential slow onset of DPA antagonism of the GABA current. Our model predicts 5 binding sites for DPA in each pentameric GABAρ1 receptor, with one per subunit. Although we do not know how many DPA molecules are required to inhibit the receptor, we hypothesize that a) the open probability of

Molecular Pharmacology Fast Forward. Published on February 11, 2016 as DOI: 10.1124/mol.116.103432
This article has not been copyedited and formatted. The final version may differ from this version.

GABAρ1 is negatively correlated with the number of DPA molecules bound to the receptor and b) the affinity of available binding sites for DPA is progressively reduced after each site is occupied by additional DPA molecules. This negative cooperativity between binding sites for DPA would also contribute to the complex recovery effects of GABAρ1. The presence of a post-DPA current tail indicates that a fraction of DPA inhibition is relieved faster than the deactivation of GABAρ1 channels, thus generating faster K_{off} than 0.18 s^{-1} (Chang and Weiss, 1999); however, the slow recovery of DPA effects also suggests that at least one additional substantially slower K_{off} exists for DPA dissociation. Notably, although the mechanism of DPA-mediated antagonism is likely distinct from that of picrotoxin antagonism, the post-DPA tail current of GABAρ1 occurs in a highly similar fashion to the post-picrotoxin tail current described for perch GABAρ1 (Qian et al., 2005). Future determination of the constant rates for DPA inhibition and equilibrium modeling may help to decipher the sequential states of DPA binding to GABAρ1; however, based on the results using BSA, realistic models should contemplate the kinetics of DPA partitioning-departitioning in the cell membrane.

DPA antagonism reduced GABA efficacy and produced a right-shift displacement of the concentration response curve; because affinity is influenced by the gating of the receptor (Chang and Weiss, 1999; Colquhoun, 1998) at this stage, we cannot discard the possibility that conformational changes affecting the affinity for GABA participate in DPA-mediated inhibition of GABA responses. However, a single point mutation of W475 generates GABA receptors with very distinct apparent affinities and distinct decay times. The measurement of binding and activity in the same oocyte demonstrated that the slow decay of the GABA current in GABAρ1 results from the lock-on of bound GABA while the receptor is in the open state (Chang and Weiss, 1999). If the same mechanism is preserved in the mutants studied here, a faster decay of

Molecular Pharmacology Fast Forward. Published on February 11, 2016 as DOI: 10.1124/mol.116.103432
This article has not been copyedited and formatted. The final version may differ from this version.

the GABA current would reflect a faster transition of GABAρ1 from the active to the closed state. Because previous studies have already demonstrated that a reduction of the channel opening rate may lead to larger EC_{50} values and lower efficacy (Chang et al., 2000), we hypothesize that mutants with faster decays will display higher GABA EC_{50} values and lower efficacy. Indeed, Figure 8 shows a linear correlation between the time constant of GABA current decay and the EC_{50} for GABA. Moreover, the maximal response to GABA was reduced by several fold in all W475 mutants (Table 1). Because the post-DPA tail and decay time are correlated, we also analyzed the relationship between the post-DPA tail and the EC_{50} for GABA. Interestingly, the amplitude of the post-DPA tail, in terms of the percentage of the maximal current, fell exponentially with increases in the apparent GABA affinity of the receptor (Fig. 8B). The Hill coefficient was negatively correlated with EC_{50} in the mutants, which can be interpreted as a reduction in the cooperativity produced by alterations in gating. Interestingly, only the W475A mutant exhibited a reduction in DPA antagonism, and we did not find any correlation between the % of antagonism and any of the kinetic or pharmacological parameters studied here (Supplemental Table 1). Evidently, W475 is a very important residue for gating transduction of the channel, substitution of polar residues renders non-functional receptors and point mutations produces channels with varied characteristics. While it is not surprising that DPA inhibition was not affected by W475F and W475L mutants, as they are very similar to W475 in terms of hydrophobicity and steric effect, the differential effects Ala and Gly substitution at the 475 position are puzzling. Both residues are small, hydrophobic and compatible with the accommodation of DPA in the transmembrane domain, thus differences in size are not a compelling reason to explain the differential effect on DPA antagonism; however, it is known that Ala and Gly are at opposite extremes of their capacity to bury hydrophobic area

Molecular Pharmacology Fast Forward. Published on February 11, 2016 as DOI: 10.1124/mol.116.103432
This article has not been copyedited and formatted. The final version may differ from this version.

within α-helical structures (Scott et al., 2007). It may be possible that Ala reduces the general hydrophobicity of DPA pocket, compared to Gly, reducing the stabilization of the DPA molecule and decreasing the antagonism of the receptor.

Taken together, the results suggest to us that the DPA-mediated antagonism of GABAρ1 results mainly from alterations in receptor gating via interactions with amino acids forming a hydrophobic cavity in the upper part of the channel. This cavity appears to be conserved in members of the Cys-loop LGIC family and would be equivalent to the hydrophobic pocket near the interphase of the membrane and the extracellular domain that was identified by photolabeling and nuclear magnetic resonance (NMR) in nAChRs (Bondarenko et al., 2013; Chiara et al., 2009) and by electron paramagnetic resonance (EPR) spectroscopy and X-ray crystallography in the prokaryotic GLIC (Nury et al., 2011; Velisetty and Chakrapani, 2012).

Molecular Pharmacology Fast Forward. Published on February 11, 2016 as DOI: 10.1124/mol.116.103432
This article has not been copyedited and formatted. The final version may differ from this version.

Acknowledgments.

We are thankful to Dr. Quoc Thang Nguyen for providing us with some DPA and with Dr. Hamish Mehaffey for critical reading of the manuscript. The authors declare no competing financial interests.

Authorship contributions.

Participated in research design: Limon, Estrada-Mondragon, Reyes-Ruiz.

Conducted experiments: Limon, Estrada Mondragon.

Contributed new reagents or analytic tools: Reyes-Ruiz, Miledi.

Performed data analysis: Limon, Estrada Mondragon.

Wrote or contributed to the writing of the manuscript: Limon, Estrada-Mondragon, Reyes-Ruiz, Miledi.

Molecular Pharmacology Fast Forward. Published on February 11, 2016 as DOI: 10.1124/mol.116.103432
This article has not been copyedited and formatted. The final version may differ from this version.

References

Akk G, Bracamontes J and Steinbach JH (2001) Pregnenolone sulfate block of GABA(A) receptors: mechanism and involvement of a residue in the M2 region of the alpha subunit. *J Physiol* **532**(Pt 3):673-684.

Bondarenko V, Mowrey D, Liu LT, Xu Y and Tang P (2013) NMR resolved multiple anesthetic binding sites in the TM domains of the alpha4beta2 nAChR. *Biochim Biophys Acta* **1828**(2):398-404.

Bouzat C, Bartos M, Corradi J and Sine SM (2008) The interface between extracellular and transmembrane domains of homomeric Cys-loop receptors governs open-channel lifetime and rate of desensitization. *J Neurosci* **28**(31):7808-7819.

Bradley J, Luo R, Otis TS and DiGregorio DA (2009) Submillisecond optical reporting of membrane potential in situ using a neuronal tracer dye. *J Neurosci* **29**(29):9197-9209.

Chanda B, Blunck R, Faria LC, Schweizer FE, Mody I and Bezanilla F (2005) A hybrid approach to measuring electrical activity in genetically specified neurons. *Nat Neurosci* **8**(11):1619-1626.

Chang Y, Covey DF and Weiss DS (2000) Correlation of the apparent affinities and efficacies of gamma-aminobutyric acid(C) receptor agonists. *Mol Pharmacol* **58**(6):1375-1380.

Chang Y and Weiss DS (1999) Channel opening locks agonist onto the GABAC receptor. *Nat Neurosci* **2**(3):219-225.

Chen H, Lyne PD, Giordanetto F, Lovell T and Li J (2006) On evaluating molecular-docking methods for pose prediction and enrichment factors. *J Chem Inf Model* **46**(1):401-415.

Chiara DC, Hamouda AK, Ziebell MR, Mejia LA, Garcia G, 3rd and Cohen JB (2009) [(3)H]chlorpromazine photolabeling of the torpedo nicotinic acetylcholine receptor identifies two state-dependent binding sites in the ion channel. *Biochemistry* **48**(42):10066-10077.

Chisari M, Wu K, Zorumski CF and Mennerick S (2011) Hydrophobic anions potently and uncompetitively antagonize GABA(A) receptor function in the absence of a conventional binding site. *Br J Pharmacol* **164**(2b):667-680.

Colquhoun D (1998) Binding, gating, affinity and efficacy: the interpretation of structure-activity relationships for agonists and of the effects of mutating receptors. *Br J Pharmacol* **125**(5):924-947.

daCosta CJ, Medaglia SA, Lavigne N, Wang S, Carswell CL and Baenziger JE (2009) Anionic lipids allosterically modulate multiple nicotinic acetylcholine receptor conformational equilibria. *J Biol Chem* **284**(49):33841-33849.

Demuro A, Martinez-Torres A, Francesconi W and Miledi R (1999) Antagonistic action of pitrazepin on human and rat GABA(A) receptors. *Br J Pharmacol* **127**(1):57-64.

Dey R and Chen L (2011) In search of allosteric modulators of a7-nAChR by solvent density guided virtual screening. *J Biomol Struct Dyn* **28**(5):695-715.

Estrada-Mondragon A and Lynch JW (2015) Functional characterization of ivermectin binding sites in alpha1beta2gamma2L GABA(A) receptors. *Front Mol Neurosci* **8**:55.

Estrada-Mondragon A, Reyes-Ruiz JM, Martinez-Torres A and Miledi R (2010) Structure-function study of the fourth transmembrane segment of the GABArho1 receptor. *Proc Natl Acad Sci U S A* **107**(41):17780-17784.

Fernandez Nievas GA, Barrantes FJ and Antollini SS (2008) Modulation of nicotinic acetylcholine receptor conformational state by free fatty acids and steroids. *J Biol Chem* **283**(31):21478-21486.

Hu XQ and Peoples RW (2008) Arginine 246 of the pretransmembrane domain 1 region alters 2,2,2-trichloroethanol action in the 5-hydroxytryptamine3A receptor. *J Pharmacol Exp Ther* **324**(3):1011-1018.

Hu XQ, Zhang L, Stewart RR and Weight FF (2003) Arginine 222 in the pre-transmembrane domain 1 of 5-HT3A receptors links agonist binding to channel gating. *J Biol Chem* **278**(47):46583-46589.

Kleijn WB, Bruner LJ, Midland MM and Wisniewski J (1983) Hydrophobic ion probe studies of membrane dipole potentials. *Biochim Biophys Acta* **727**(2):357-366.

Lee WY, Free CR and Sine SM (2009) Binding to gating transduction in nicotinic receptors: Cys-loop energetically couples to pre-M1 and M2-M3 regions. *J Neurosci* **29**(10):3189-3199.

Limon A, Reyes-Ruiz JM, Vaswani RG, Chamberlin AR and Miledi R (2010) Kaitocephalin antagonism of glutamate receptors expressed in Xenopus oocytes. *ACS Chem Neurosci* **1**(3):175-181.

Linsenbardt AJ, Chisari M, Yu A, Shu HJ, Zorumski CF and Mennerick S (2012) Noncompetitive, voltage-dependent NMDA receptor antagonism by hydrophobic anions. *Mol Pharmacol* **83**(2):354-366.

Martinez-Delgado G, Estrada-Mondragon A, Miledi R and Martinez-Torres A (2010) An Update on GABArho Receptors. *Curr Neuropharmacol* **8**(4):422-433.

Martinez-Torres A, Vazquez AE, Panicker MM and Miledi R (1998) Cloning and functional expression of alternative spliced variants of the rho1 gamma-aminobutyrate receptor. *Proc Natl Acad Sci U S A* **95**(7):4019-4022.

Mennerick S, Lamberta M, Shu HJ, Hogins J, Wang C, Covey DF, Eisenman LN and Zorumski CF (2008) Effects on membrane capacitance of steroids with antagonist properties at GABAA receptors. *Biophys J* **95**(1):176-185.

Miledi R (1982) A calcium-dependent transient outward current in Xenopus laevis oocytes. *Proc R Soc Lond B Biol Sci* **215**(1201):491-497.

Miledi R, Palma E and Eusebi F (2006) Microtransplantation of neurotransmitter receptors from cells to Xenopus oocyte membranes: new procedure for ion channel studies. *Methods Mol Biol* **322**:347-355.

Miller PS and Aricescu AR (2014) Crystal structure of a human GABAA receptor. *Nature* **512**(7514):270-275.

Nury H, Van Renterghem C, Weng Y, Tran A, Baaden M, Dufresne V, Changeux JP, Sonner JM, Delarue M and Corringer PJ (2011) X-ray structures of general anaesthetics bound to a pentameric ligand-gated ion channel. *Nature* **469**(7330):428-431.

Oberhauser AF and Fernandez JM (1995) Hydrophobic ions amplify the capacitive currents used to measure exocytotic fusion. *Biophys J* **69**(2):451-459.

Ochoa-de la Paz LD, Estrada-Mondragon A, Limon A, Miledi R and Martinez-Torres A (2012) Dopamine and serotonin modulate human GABArho1 receptors expressed in Xenopus laevis oocytes. *ACS Chem Neurosci* **3**(2):96-104.

Prevost MS, Sauguet L, Nury H, Van Renterghem C, Huon C, Poitevin F, Baaden M, Delarue M and Corringer PJ (2012) A locally closed conformation of a bacterial pentameric proton-gated ion channel. *Nat Struct Mol Biol* **19**(6):642-649.

Qian H, Pan Y, Zhu Y and Khalili P (2005) Picrotoxin accelerates relaxation of GABAC receptors. *Mol Pharmacol* **67**(2):470-479.

Reeves DC, Jansen M, Bali M, Lemster T and Akabas MH (2005) A role for the beta 1-beta 2 loop in the gating of 5-HT3 receptors. *J Neurosci* **25**(41):9358-9366.

Reyes-Ruiz JM, Ochoa-de la Paz LD, Martinez-Torres A and Miledi R (2010) Functional impact of serial deletions at the C-terminus of the human GABArho1 receptor. *Biochim Biophys Acta* **1798**(5):1002-1007.

Sali A and Blundell TL (1993) Comparative protein modelling by satisfaction of spatial restraints. *J Mol Biol* **234**(3):779-815.

Scott KA, Alonso DO, Sato S, Fersht AR and Daggett V (2007) Conformational entropy of alanine versus glycine in protein denatured states. *Proc Natl Acad Sci U S A* **104**(8):2661-2666.

Molecular Pharmacology Fast Forward. Published on February 11, 2016 as DOI: 10.1124/mol.116.103432
This article has not been copyedited and formatted. The final version may differ from this version.

Totrov M and Abagyan R (1997) Flexible protein-ligand docking by global energy optimization in internal coordinates. *Proteins* **Suppl 1**:215-220.

Unwin N and Fujiyoshi Y (2012) Gating movement of acetylcholine receptor caught by plunge-freezing. *J Mol Biol* **422**(5):617-634.

Velisetty P and Chakrapani S (2012) Desensitization mechanism in prokaryotic ligand-gated ion channel. *J Biol Chem* **287**(22):18467-18477.

Wang CC and Bruner LJ (1978) Lipid-dependent and phloretin-induced modifications of dipicrylamine adsorption by bilayer membranes. *Nature* **272**(5650):268-270.

Molecular Pharmacology Fast Forward. Published on February 11, 2016 as DOI: 10.1124/mol.116.103432
This article has not been copyedited and formatted. The final version may differ from this version.

Footnotes

a) This work was supported by King Abdul Aziz City for Science and Technology, Saudi Arabia [grant KACST-46749] and The University of California Institute for Mexico and United States (UC-MEXUS) [grant CN-13-613].

b) Part of this work was presented at the Society for Neuroscience 2013 meeting.

c) Agenor Limon. alimonru@uci.edu; 2226 Gillespie Neuroscience Research Facility, Irvine CA 92697.

Molecular Pharmacology Fast Forward. Published on February 11, 2016 as DOI: 10.1124/mol.116.103432
This article has not been copyedited and formatted. The final version may differ from this version.

Legends for Figures

Figure 1. Concentration dependent antagonism of DPA on $GABA_A$Rs. A. Effect of 1 mM GABA plus 100 nM DPA coapplication on $GABA_A$Rs expressed by mRNA-injected oocytes. B**.** Concentration-dependent antagonism of GABAρ1 receptors by DPA. C, Inhibition curves of DPA on $GABA_A$Rs (1 mM GABA) and GABAρ1 (100 µM GABA). No DPA preincubation was used for the experiments shown in A-C. IC_{50} was 1.57 ± 0.2 µM for GABAρ1 (n = 4 oocytes) and 62 ± 11 nM for $GABA_A$Rs (n = 3-5 oocytes per concentration).

Figure 2. Non-competitive antagonism of DPA. A. Ion currents elicited by sequential increments of GABA concentration in absence and presence of 3 µM DPA. B. Concentration and maximal GABA currents relationship in absence and presence of 3 µM DPA. Notice that 5 µM DPA (black triangle), without preincubation, did not further reduce the fast peak of the GABA current. This indicates that without DPA preincubation the onset of DPA antagonism is always slower than the activation of GABA current. In contrast, three minutes preincubation with 3 µM DPA produced (white circles) produced a stronger, unsurmountable antagonism of GABAρ1, and three minutes preincubation with 5 µM (preDPA) reduced almost completely the maximum GABA current (white triangle at lowest right corner in the graph). Each data point is the mean ± S.E.M. of 3-6 oocytes. To avoid cumulative DPA effects only one application per oocyte was used.

Figure 3. Slow onset of DPA antagonism of GABAρ1. A. Representative GABAρ1 currents showing the effect of the DPA preincubation time on the activation of the current. B. Plot of the mean ± S.E.M. of 6 single tested oocytes per point. C, D. DPA antagonism offset in presence of GABA can be described by a single exponential function with a time constant τ of 36.2 ± 5.3 s.

Molecular Pharmacology Fast Forward. Published on February 11, 2016 as DOI: 10.1124/mol.116.103432
This article has not been copyedited and formatted. The final version may differ from this version.

BSA, a known scavenger of DPA, accelerated the τ of antagonism offset to 16.8 ± 1.7 s (p = 0.014; n = 4 oocytes) and facilitated the complete recovery of DPA antagonism upon repeated DPA applications.

Figure 4. Voltage dependence of DPA antagonism. A. DPA-induced charge movements were obtained in non-injected oocytes by applying voltage pulses from a holding potential of -90 mV to voltages between -120 to +60 mV in 10 mV steps. Traces shown in the insert were obtained by subtracting the capacitive currents in control conditions from those in presence of DPA after 3 minutes incubation. Normalized voltage dependence of DPA charge is best described by a Boltzmann equation of the form $1/[1 + \exp(V_{1/2} - V)/S]$, where $V_{1/2}$ is the half voltage for maximum charge, V is the test potential and S is the slope factor. In our experiments DPA's $V_{1/2}$ was -55 ± 2.3 mV with an S of 32.8 ± 2.5 (n = 6). B. Representative currents elicited by the ramp protocol shown in the insert. Steady-state 1 mM GABA current was obtained by subtracting the current elicited by the ramp protocol in control conditions from the ramp-elicited current after the response to 1 μM GABA reached the equilibrium. The GABA-current not blocked by 3 μM DPA was determined by subtracting ramp-elicited currents before and after 200 s incubation with DPA. C. Voltage dependence of mean fractional steady state GABA currents (dark line) available after 200 ms of DPA ± S.E.M (gray area; n = 5). Asymptotic values around the inversion potential of GABA current were omitted from the plot. D. Percentage of block at two values of voltage. E. GABA currents elicited by 1 μM GABA on oocytes clamped at negative and positive voltages. F-G. Plot of the time constants of the antagonist effect of DPA at different voltages. *** $p < 0.001$, * $p < 0.05$.

Figure 5. Differential effects of DPA on Cys-loop LGIC. Five μM DPA was preincubated for 180 s to allow adequate membrane partition. Homomeric GABAρ1, nAChα7 and 5-HT_{3A}

Molecular Pharmacology Fast Forward. Published on February 11, 2016 as DOI: 10.1124/mol.116.103432
This article has not been copyedited and formatted. The final version may differ from this version.

receptors were activated by 100 µM GABA, 100 µM ACh and 10 µM 5-HT, respectively. Notice that 5-HT_{3A} receptors were not affected by high concentrations of DPA.

Figure 6. Docking of DPA on Cys-loop homomeric receptors. Left, Structural model of GABAρ1 interacting with DPA, the hydrophobic interaction with DPA hinders the appropriate communication of the transmembrane domains with the extracellular compartments disturbing the conformational change in the gating. Center, nAChRα7, the additional non-covalent contacts between DPA and the Cys-loop domain potentiate the activation of the channel. Right, 5-HT_{3A}, the loose hydrophobic interactions do not modify significantly the function of the channel.

Figure 7. Mutational analysis of GABAρ1 and DPA antagonism. Sequential reduction of the M4 and substitution of the W475 residue produced GABA receptors with distinct kinetic properties (see Table 1 for details). To evaluate DPA antagonism on the mutants, 1 µM DPA was pre-incubated for 180 s and then an EC_{50} concentration of GABA was co-applied DPA. Notice the changes in the post-DPA relaxation. The removal of -3aa in the C-termini of the M4 modestly enhanced the antagonistic effect of DPA. In contrast the substitution of W475A, a substitution of an amino acid with different hydrophobicity, reduced DPA effects. C. Percentage of inhibition by DPA of the GABA-currents elicited by the different mutants studied. E. Full dose response for W475A, W475F and WT shows a larger IC_{50} for W475A.

Figure 8. Analysis of correlation between the pharmacological and kinetic measures of W475 mutants. A, Time constant of current decay is faster in the mutants which also show reduced apparent affinity for GABA. B. The tail relaxation observed at the end of DPA perfusion follows a single exponential relationship with the affinity for GABA of the receptors. C. The mutants show a reduction of cooperativity, with changes in the Hill coefficient to near 1 in most of the

Molecular Pharmacology Fast Forward. Published on February 11, 2016 as DOI: 10.1124/mol.116.103432
This article has not been copyedited and formatted. The final version may differ from this version.

cases. The percentage of DPA inhibition did not show a clear relationship with the EC_{50}. All data are Mean ± SEM. The lines in A and B are the linear and exponential fit to the experimental data. The coefficient of correlation for each curve is shown as insert.

Molecular Pharmacology Fast Forward. Published on February 11, 2016 as DOI: 10.1124/mol.116.103432
This article has not been copyedited and formatted. The final version may differ from this version.

Table 1. Properties of GABAρ1 mutants

Receptor	N	EC_{50} (μM) for GABA	Hill	N	GABA current at the [EC_{50}] (nA)	Tau of current activation (s)	Tau of current decay (s)
WT	5	0.73 ± 0.14	3.0 ± 0.5	6	3945 ± 206	5.1 ± 2.8	22.1 ± 0.8
-1aa	3	0.41 ± 0.05	3.0 ± 0.1	6	2279 ± 479***	11.6 ± 0.8***	28.2 ± 0.9***
-2aa	3	2.16 ± 0.06**	3.9 ± 0.7	6	5246 ±109***	2.4 ± 0.1**	6.2 ± 0.1 ***
-3aa	3	1.26 ± 0.15	1.4 ± 0.1**	6	604 ± 129***	7.1 ± 0.1*	22.8 ± 0.7
W475F	12	4.08 ± 0.49***	1.6 ± 0.1**	5	879 ± 91***	3.6 ± 0.2	6.3 ± 0.4***
W475L	4	1.72 ± 0.24**	2.3 ± 0.02	5	620 ± 65***	4.5 ± 0.5	12.4 ± 0.4***
W475A	4	2.72 ± 0.35***	1.4 ± 0.2**	6	634 ± 57***	4.6 ± 1.0	11.0 ± 1.1***
W475G	4	3.30 ± 0.12 ***	1.4 ± 0.1**	5	54 ± 7***	3.5 ± 0.2	11.7 ± 1.1***
W465R	3	NR	NR	3	ND	NR	NR
W475D	3	NR	NR	3	ND	NR	NR

NR, no response to GABA; ND, no determined. Rise time is the tau activation mean ± S.E.M., of the EC_{50} current. Statistical comparison using Dunnett's method.* $p < 0.05$, ** $p < 0.005$, *** $p < 0.0001$.

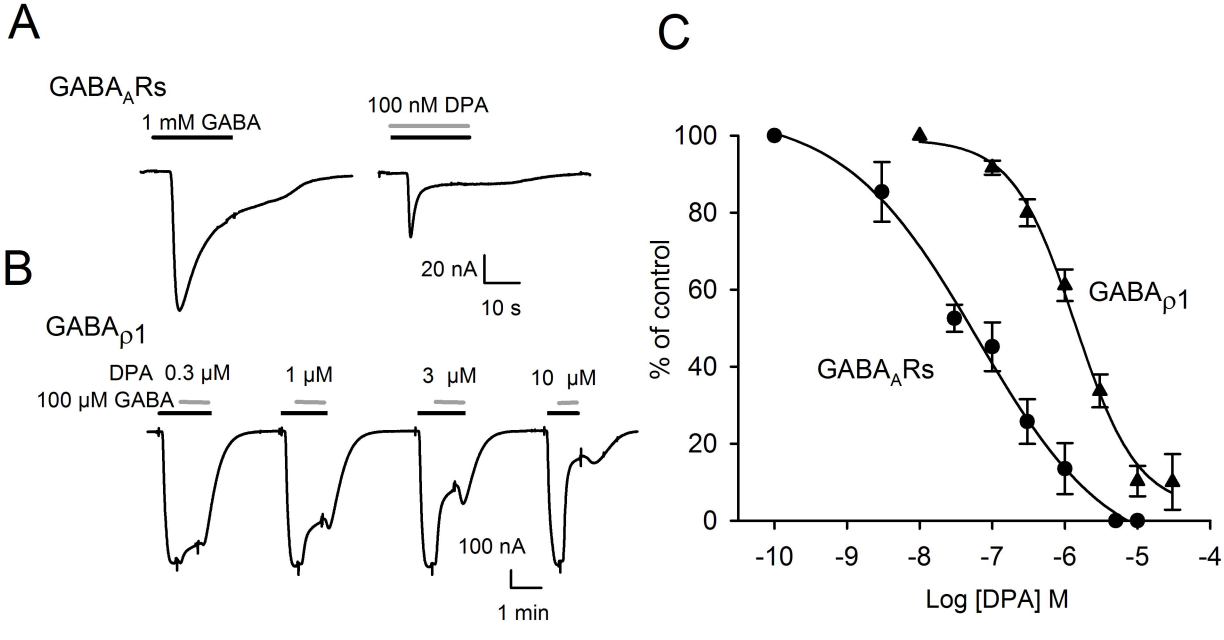
A
GABA$_A$Rs
1 mM GABA
100 nM DPA
20 nA
10 s
B
GABA$_\rho$1
DPA 0.3 µM
1 µM
3 µM
10 µM
100 µM GABA
100 nA
1 min
C
% of control
100
80
60
40
20
0
-10
-9
-8
-7
-6
-5
-4
Log [DPA] M
GABA$_\rho$1
GABA$_A$Rs

Figure 1

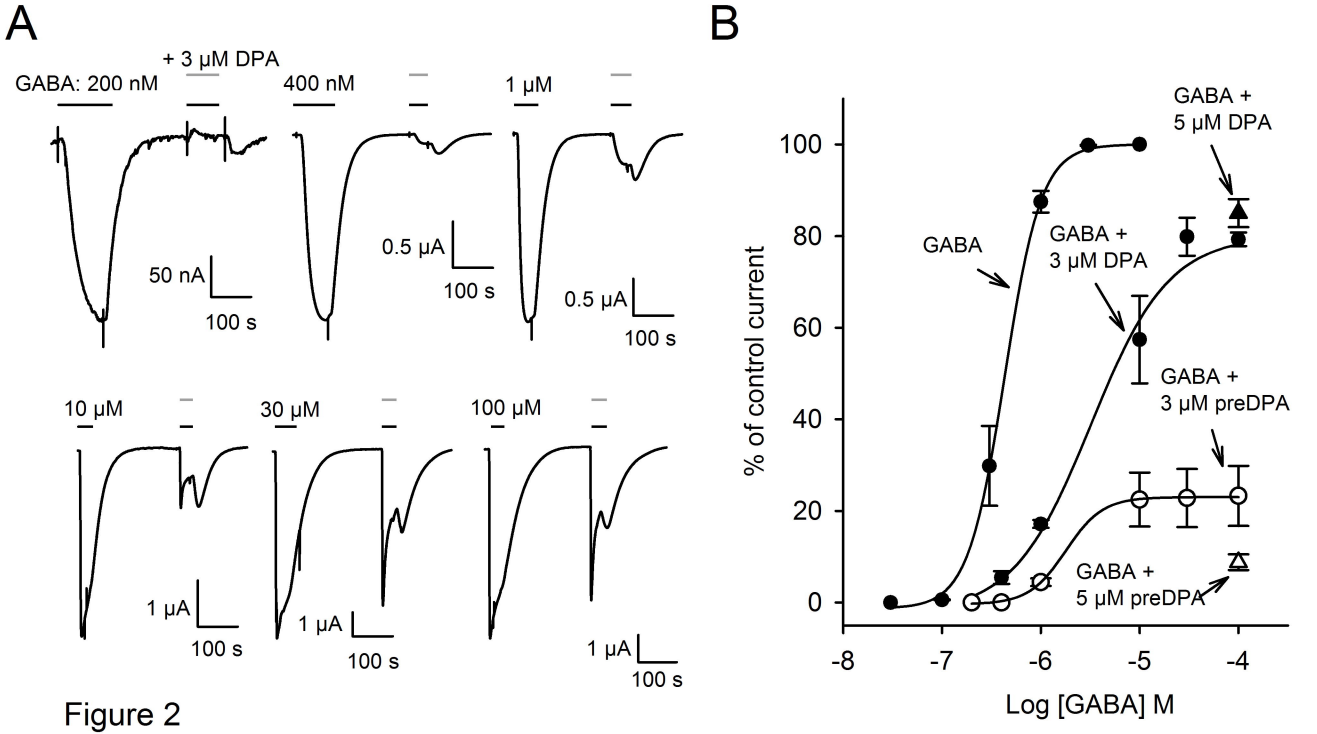
A
+ 3 μM DPA
GABA: 200 nM
400 nM
1 μM
50 nA
100 s
0.5 μA
100 s
0.5 μA
100 s
10 μM
30 μM
100 μM
1 μA
100 s
1 μA
100 s
1 μA
100 s
B
GABA +
5 μM DPA
GABA
GABA +
3 μM DPA
GABA +
3 μM preDPA
GABA +
5 μM preDPA
% of control current
100
80
60
40
20
0
-8
-7
-6
-5
-4
Log [GABA] M

Figure 2

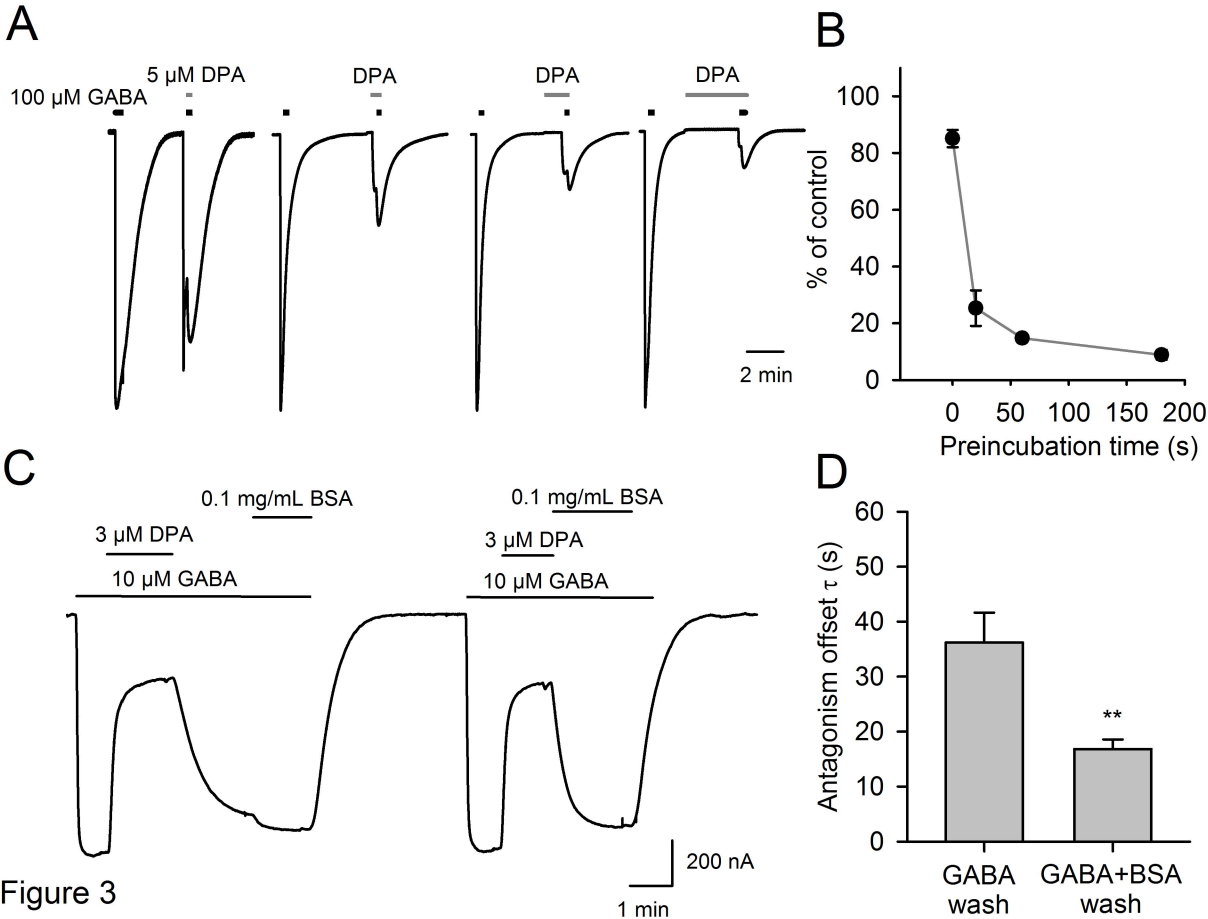
A
5 μM DPA
DPA
DPA
DPA
100 μM GABA
2 min
B
% of control
100
80
60
40
20
0
0
50
100
150
200
Preincubation time (s)
C
0.1 mg/mL BSA
0.1 mg/mL BSA
3 μM DPA
3 μM DPA
10 μM GABA
10 μM GABA
200 nA
1 min
D
Antagonism offset τ (s)
60
50
40
30
20
10
0
**
GABA wash
GABA+BSA wash

Figure 3

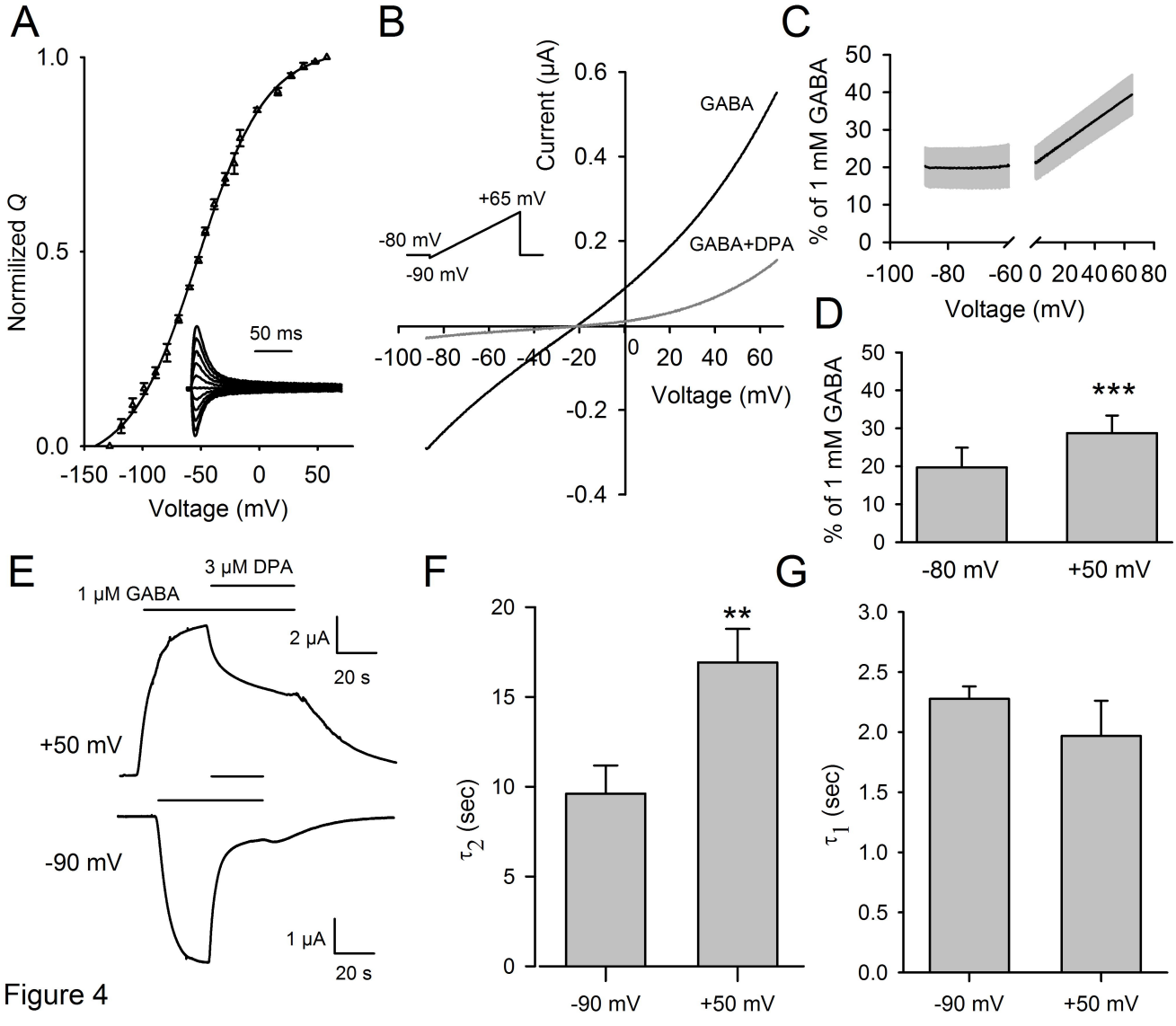
A
1.0
0.5
0.0
Normilized Q
50 ms
-150 -100 -50 0 50
Voltage (mV)
B
Current (μA)
0.6
0.4
0.2
-0.2
-0.4
GABA
GABA+DPA
+65 mV
-80 mV
-90 mV
-100 -80 -60 -40 -20 0 20 40 60
Voltage (mV)
C
% of 1 mM GABA
50
40
30
20
10
0
-100 -80 -60 0 20 40 60 80
Voltage (mV)
D
% of 1 mM GABA
***
-80 mV
+50 mV
E
3 μM DPA
1 μM GABA
2 μA
20 s
+50 mV
-90 mV
1 μA
20 s
F
τ2 (sec)
**
-90 mV
+50 mV
G
τ1 (sec)
3.0
2.5
2.0
1.5
1.0
0.5
0.0
-90 mV
+50 mV

Figure 4

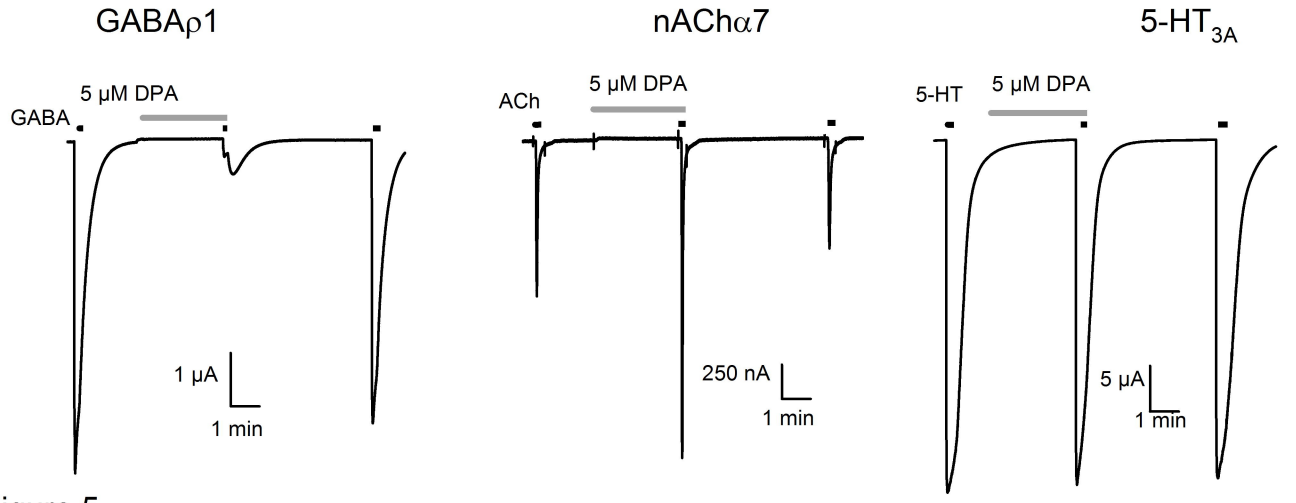
GABAρ1
5 μM DPA
GABA
1 μA
1 min
nAChα7
ACh
5 μM DPA
250 nA
1 min
5-HT3A
5-HT
5 μM DPA
5 μA
1 min

Figure 5

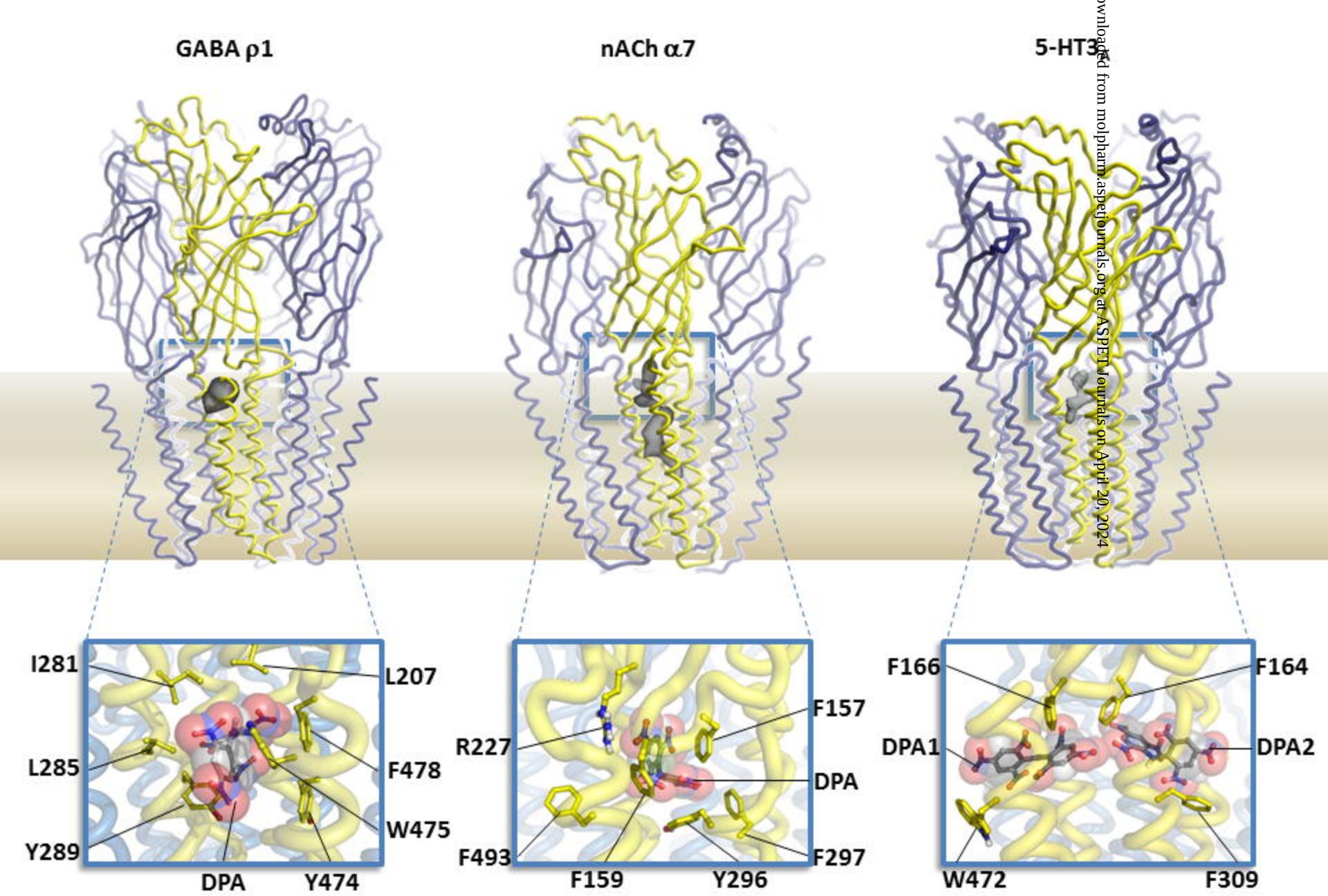

Figure 6

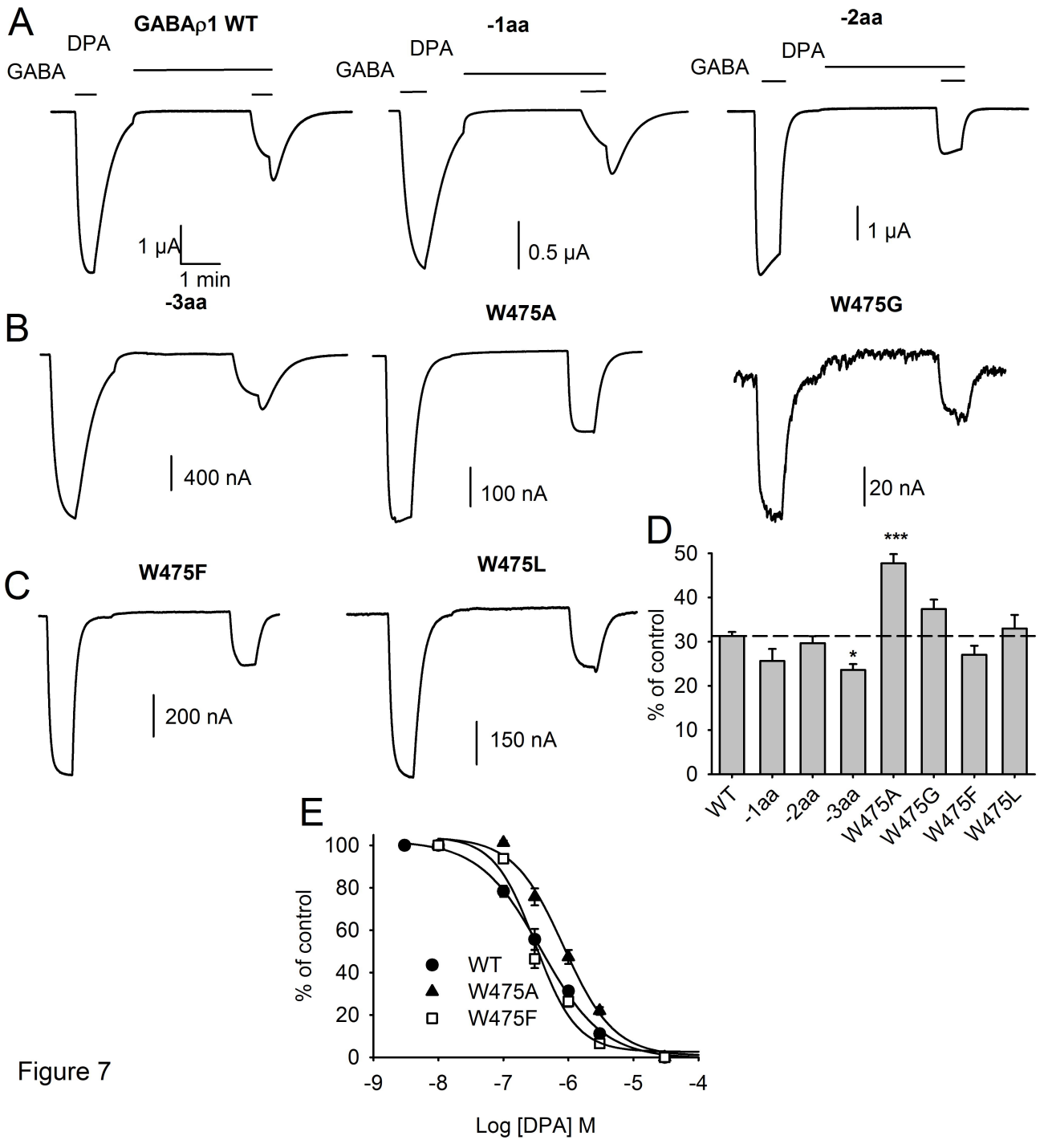
A
GABAρ1 WT
DPA
GABA
1 μA
1 min
-1aa
0.5 μA
-2aa
1 μA
B
-3aa
400 nA
W475A
100 nA
W475G
20 nA
C
W475F
200 nA
W475L
150 nA
D
% of control
***
*
WT
-1aa
-2aa
-3aa
W475A
W475G
W475F
W475L
E
% of control
WT
W475A
W475F
Log [DPA] M

Figure 7

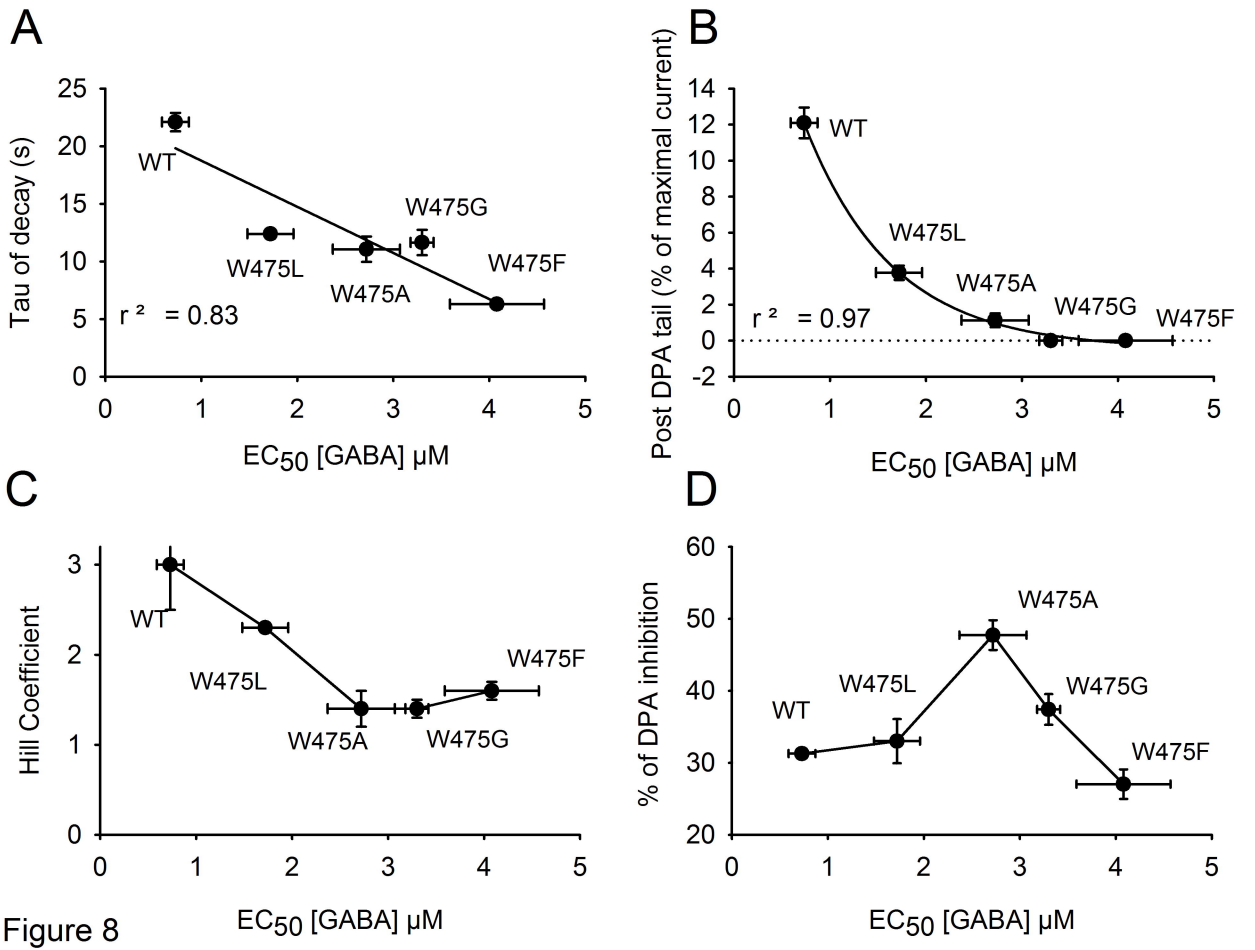
A
Tau of decay (s)
25
20
15
10
5
0
WT
W475L
W475A
W475G
W475F
r² = 0.83
0
1
2
3
4
5
EC50 [GABA] µM
B
Post DPA tail (% of maximal current)
14
12
10
8
6
4
2
0
-2
WT
W475L
W475A
W475G
W475F
r² = 0.97
EC50 [GABA] µM
C
Hill Coefficient
3
2
1
0
WT
W475L
W475A
W475G
W475F
EC50 [GABA] µM
D
% of DPA inhibition
60
50
40
30
20
WT
W475L
W475A
W475G
W475F
EC50 [GABA] µM

Figure 8